JOC The Journal of Organic Chemistry

Article

pubs.acs.org/joc

Experimental and Theoretical Analyses of Azulene Synthesis from Tropones and Active Methylene Compounds: Reaction of 2-Methoxytropone and Malononitrile

Takahisa Machiguchi,[†] Toshio Hasegawa,[†] Shinichi Yamabe,[‡] Tsutomu Minato,*[,§] Shoko Yamazaki,[‡] and Tetsuo Nozoe[∥]

[†]Department of Chemistry, Faculty of Science, Saitama University, 255 Shimo-Ohkubo, Saitama 338-8570, Japan

[‡]Department of Chemistry, Nara University of Education, Takabatake-cho, Nara 630-8528, Japan

[§]Institute for Natural Science, Nara University, Misasagi-cho, Nara 631-8502, Japan

[∥]Tokyo Research Laboratories, Kao Corporation, Bunka, Sumida-ku, Tokyo 131-8501, Japan

Supporting Information

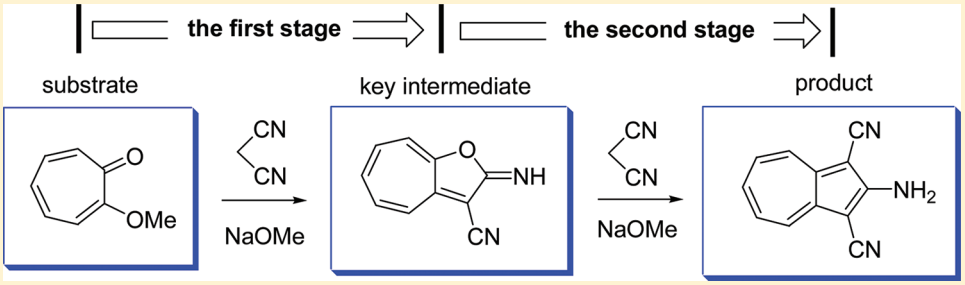

ABSTRACT: A representative azulene formation from an active troponoid precursor (2-methoxytropone) and an active methylene compound (malononitrile) has been analyzed both experimentally and theoretically. ^{2}H-Tracer experiments using 2-methoxy[3,5,7-$^2H_3$]tropone (**2**-d_3) and malononitrile anion give 2-amino-1,3-dicyano[4,6,8-$^2H_3$]azulene (**1**-d_3) in quantitative yield. New and stable ^{2}H-incorporated reaction intermediates have been isolated, and main intermediates have been detected by careful low-temperature NMR measurements. The detection has been guided by mechanistic considerations and B3LYP/6-31(+)G(d) calculations. The facile and quantitative one-pot formation of azulene **1** has been found to consist of a number of consecutive elementary processes: (a) The troponoid substrate, 2-methoxytropone (**2**), is subject to a nucleophilic substitution by the attack of malononitrile anion ($HC(CN)_2^-$) to form a Meisenheimer-type complex **3**, which is rapidly converted to 2-troponylmalononitrile anion (**5**). (b) The anion **5** is converted to an isolable intermediate, 2-imino-2*H*-cyclohepta[*b*]furan-3-carbonitrile (**6**), by the first ring closure in the reaction. (c) A nucleophilic addition of the second $HC(CN)_2^-$ toward the imine **6** at the C-8a position produces the second Meisenheimer-type adduct **7**. (d) The second ring closure leads to 1-carbamoyl-1,3-dicyano-2-imino-2,3-dihydroazulene (**11**). A base attacks the imine **11**, which results in generation of a conjugate base **12** of the final product, azulene **1**.

INTRODUCTION

A name of *azulene*[1] appeared over 100 years ago and originated from its color (blue, azure), without knowledge of its properties and composition. Owing to its beautiful color and the aromatic character,[2] the natural azulene pigments[3] have been studied extensively, especially after the first synthesis of azulenes by Pfau and Plattner.[4] The parent azulene, its derivatives, and azulenequinones[5,6] have attracted considerable interest of many organic chemists.[7,8] Hence, a large number of azulene syntheses have been reported. However, most of these methods involve a final dehydrogenation step at high temperatures (250–300 °C). Accordingly, the yield of azulene in general is inevitably very low.[1,2] Nowadays, two general and convenient methods for azulene synthesis *without involving the dehydrogenation step* are known. They appeared in 1955 simultaneously. One is a Hafner's elegant method shown in Scheme 1.[9−11] The method is very useful[10,11] for preparation of the parent azulene and its homologues bearing substituents in the seven-membered ring.

The other method is the Nozoe azulene synthesis whose name was initially used by McDonald and Richmond.[12] This general synthesis was devised[13] and has been developed by one of the present authors (T.N.) and his co-workers.[14] Scheme 2 shows the reactions of this efficient formation of polyfunctional azulene derivatives from reactive troponoid and active methylene compounds such as malononitrile (MLN). It is surprising that such heavily substituted azulenes are produced without any difficulty in one-pot reactions and with high yields.

Received: April 5, 2012
Published: May 22, 2012

dx.doi.org/10.1021/jo300693n | J. Org. Chem. 2012, 77, 5318–5330

Scheme 1. An Example of Hafner's Azulene Synthesis[a]

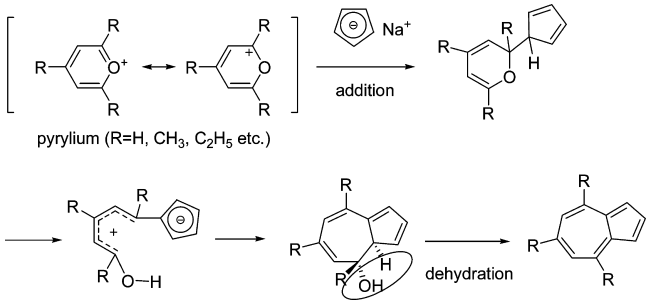

[a]See refs 9−11.

Scheme 2. General and Facile Formation of Polyfunctional Azulenes (Nozoe Azulene Synthesis[12]) from the Reaction between Troponoid Substrates and Active Methylene Compounds[a]

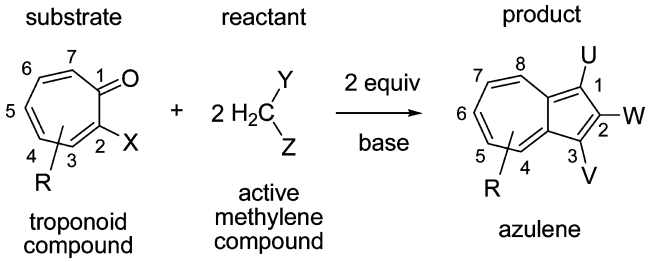

R = alkyl (Me, Et, ^{i}Pr etc)
X = Cl, Br, or $OSO_2C_6H_4$-*p*-Me
Y, Z, U, V = CN, $CONH_2$, CO_2Et, CO_2Me, or COMe
W = NH_2 or OH

R = H X = OMe	Y = Z = CN	U = V = CN W = NH_2
(**2**)	(MLN)	(**1**)
		studied in this work

[a]See refs 13−15.

Nozoe azulene synthesis has great advantages in the easy preparation of azulenes with versatile amino and hydroxy groups (W in Scheme 2) at the C-2 position. These groups cannot be introduced to azulene skeleton by any other means. Hence, the two methods in Schemes 1 and 2 are complementary to each other. The amino (or hydroxyl) group at the C-2 position of the azulene strongly activates the C-4, C-6, and C-8 positions for electrophilic substitutions. Also, cyano (or alkoxycarbonyl) groups at C-1 and C-3 positions of the azulene activate strongly the C-4, C-6, and C-8 positions for electrophilic reactions and activate strongly the C-5, C-7, and C-2 positions for nucleophilic reactions. Hence, these trifunctional azulenes can be converted to many other azulenes including the parent azulene. This is the major advantage of the method in Scheme 2. However, its reaction mechanism has been veiled for a long time.

We would like to elucidate here a mechanism of this remarkably facile formation of azulene derivatives in Scheme 2. A fundamental example is formation of 2-amino-1,3-dicyanoazulene (**1**) from a troponoid ([7]annulenone) substrate (2-chlorotropone) and malononitrile (MLN) in the presence of a base. We chose 2-methoxytropone (**2**) as a substrate, since we have found that 2-chlorotropone is converted gradually to 2-methoxytropone in methanol at room temperature in the presence of NaOMe. The MeO^- conjugate ion works as a nucleophile onto either the C-2 carbon or the C-7 of the tropone ring.

RESULTS AND DISCUSSION

Experimental Analysis and Tracer Experiments Using ^{2}H-Labeled Substrate. In order to analyze reaction paths and intermediate structures precisely, we needed to prepare a ^{2}H-labeled substrate with high isotopic purity for parallel experiments with the unlabeled material. In this work, we have succeeded in obtaining the starting material, [3,5,7-$^2H_3$]-tropolone,[15−17] with *highest* achievable isotopic purity by a facile preparation by a direct deuteration of tropolone using only D_2O on heating (see Experimental Section). The $^2H_3$-labeled compound obtained led easily to the desired substrate, 2-methoxy[3,5,7-$^2H_3$]tropone (**2**-d_3) with high isotopic purity (d_3, 99.6%; d_2, 0.4%, from mass spectrometry) in high yield.

We have analyzed the reaction between 2-methoxytropone (**2**) and malononitrile (MLN), using the ^{2}H-labeled troponoid substrate, **2**-d_3. Two moles of a base (NaOMe or *t*-$BuNH_2$) and an active methylene compound, MLN, in methanol are also used in Scheme 2. The ^{13}C and ^{1}H NMR data of the substrates **2** and **2**-d_3 are shown in Tables 1A and 2A, respectively. These NMR and mass spectral data (see Experimental Section) again indicate that the substrate **2**-d_3 contains deuterium efficiently with more than 99.5% isotopic purity and selectively at the 3, 5, and 7 positions of the [7]annulenone (troponoid) skeleton.

In Scheme 2, 2 mol of reactant (MLN) and 2 equiv of base (NaOMe or *t*-$BuNH_2$) have been used.[14] When 1 mol of MLN and 1 equiv of base are adopted, an isolable and key intermediate, 2-imino-2*H*-cyclohepta[*b*]furan-3-carbonitrile (**6**), can be generated (Scheme 3). The substrate **2** reacts with the first mole of MLN in the presence of NaOMe at room temperature overnight to give 2-troponylmalononitrile anion **5**. Neutralization with dil HCl leads to the isolation of the sodium-free compound 2-imino-2*H*-cyclohepta[*b*]furan-3-carbonitrile (**6**) as orange crystals in high yield. Subsequently, addition of the second mole of MLN and 1 equiv of base to **6** gives the product, 2-amino-1,3-dicyanoazulene (**1**). Thus, it is confirmed that the key intermediate **6** intervenes at the (**2** → **1**) reaction channel. Use of the ^{2}H-labeled substrate, **2**-d_3, gives rise to an intermediate, 2-imino-2*H*-[4,6,8-$^2H_3$]cyclohepta[*b*]furan-3-carbonitrile (**6**-d_3), in Scheme 3. ^{13}C and ^{1}H NMR spectral data of **6**-d_3 are shown in Tables 1B and 2B, respectively, and those of the product **1** are in Tables 1C and 2C, respectively.

In order to observe the ^{2}H nucleus directly in the substrate (**2**), key intermediate (**6**), and product (**1**), we have performed ^{2}H NMR spectroscopy.[18] Table 3 summarizes the results. These ^{2}H NMR spectral results are consistent with ^{13}C and ^{1}H NMR data in Tables 1 and 2.

All of the NMR (^{13}C, ^{1}H, and ^{2}H) spectra demonstrate that the azulene **1**-d_3, obtained from **2**-d_3, contains deuteriums at the 4, 6, and 8 positions of **1** via 2-imino-2*H*-[4,6,8-$^2H_3$]cyclohepta[*b*]-furan-3-carbonitrile (**6**-d_3). ^{1}H NMR and ^{13}C NMR charts of **2**, **2**-d_3, **6**, **6**-d_3, **1**, and **1**-d_3 are shown in Figure S3 of Supporting Information.

In addition to the purpose of the precise assignment of ^{1}H NMR spectra, use of the ^{2}H-labeled substrate (**2**-d_3) is needed to judge whether the primary nucleophilic addition of $HC(CN)_2^-$ and elimination are through path A at C-2 (normal) or path B at C-7 (abnormal)[19] on the tropone ring (Scheme 4). The obtained

dx.doi.org/10.1021/jo300693n | J. Org. Chem. 2012, 77, 5318−5330

Table 1. Selected ^{13}C NMR (100.6 MHz) Spectral Data for (A) Substrates, (B) Key Reaction Intermediates, and (C) Product Azulenes[a]

(A) substrates, 2-methoxytropone (**2**) and 2-methoxy[3,5,7-$^2H_3$]tropone (**2**-d_3)								
compd	C(1)	C(2)	C(3)	C(4)	C(5)	C(6)	C(7)	OCH_3
2	180.33 (s)	165.29 (s)	112.24 (d)	132.51 (d)	127.68 (d)	136.36 (d)	136.71 (d)	56.11 (q)
	$^3J_{CH(6)}$ 12.0	$^3J_{CH(4)}$ 11.5	$^1J_{CH}$ 151.5	$^1J_{CH}$ 157.4	$^1J_{CH}$ 157.5	$^1J_{CH}$ 155.3	$^1J_{CH}$ 160.0	$^1J_{CH}$ 146.2
2-d_3	180.51 (s)	165.43 (s)	112.01 (t)[b]	132.38 (d)	127.51 (t)[b]	136.24 (d)	136.64 (t)[b]	56.31 (q)
	$^3J_{CH(6)}$ 12.0	$^3J_{CH(4)}$ 11.5	$^1J_{CD}$ 23.0	$^1J_{CH}$ 157.6	$^1J_{CD}$ 24.3	$^1J_{CH}$ 155.3	$^1J_{CD}$ 24.1	$^1J_{CH}$ 146.3

(B) key reaction intermediates, 2-imino-2*H*-cyclohepta[*b*]furan-3-carbonitrile (**6**) and 2-imino-2*H*-[4,6,8-$^2H_3$]cyclohepta[*b*]furan-3-carbonitrile (**6**-d_3)										
compd	C(2)	C(3)	C(3a)	C(4)	C(5)	C(6)	C(7)	C(8)	C(8a)	C≡N
6	166.97 (s)	85.41 (s)	155.56 (s)	127.60 (d)	141.15 (d)	133.50 (d)	137.63 (d)	117.29 (d)	162.20 (s)	113.54 (s)
		$^3J_{CH(4)}$ 2.5	$^3J_{CH(5)}$ 11.9	$^1J_{CH}$ 162.9	$^1J_{CH}$ 159.9	$^1J_{CH}$ 162.7	$^1J_{CH}$ 162.4	$^1J_{CH}$ 162.4	$^3J_{CH(7)}$ 11.9	
6-d_3	166.82 (s)	85.09 (s)	155.52 (s)	127.42 (t)[b]	141.11 (d)	133.33 (t)[b]	137.59 (d)	117.30 (t)[b]	162.10 (s)	113.49 (s)
			$^3J_{CH(5)}$ 11.4	$^1J_{CD}$ 24.3	$^1J_{CH}$ 159.9	$^1J_{CD}$ 24.9	$^1J_{CH}$ 162.4	$^1J_{CD}$ 25.4	$^3J_{CH(7)}$ 11.9	

(C) product azulenes, 2-amino-1,3-dicyanoazulene (**1**) and 2-amino-1,3-dicyano[4,6,8-$^2H_3$]azulene (**1**-d_3)							
compd	C(1,3)	C(2)-NH_2	C(3a,8a)	C(6)	C(5,7)	C(4,8)	C≡N
1	81.38 (s)	160.25 (s)	146.32 (s)	133.76 (d)	132.88 (d)	128.77 (d)	115.02 (s)
	$^3J_{C(1)H(8)}$ 11.6		$^3J_{C(3a)H(5)}$ 10.5	$^1J_{CH}$ 161.7	$^1J_{CH}$ 161.3	$^1J_{CH}$ 157.1	
1-d_3	81.33 (s)	160.39 (s)	146.46 (s)	133.72 (t)[b]	132.99 (d)	128.69 (t)[b]	115.32 (s)
	$^4J_{C(1)H(4)}$ 5.9		$^3J_{C(3a)H(5)}$ 10.5	$^1J_{CD}$ 24.3	$^1J_{CH}$ 161.3	$^1J_{CD}$ 23.3	

[a]For the atomic numbering of $^2H_3$-labeled species and undeuteriated compounds, see Scheme 3. Chemical shifts and coupling constants are in δ scale and Hz unit, respectively. Solvents used were $CDCl_3$, CD_3OD, and Me_2SO-d_6 for the substrates (**2** and **2**-d_3), key reaction intermediates (**6** and **6**-d_3), and product azulenes (**1** and **1**-d_3), respectively, with Me_4Si as the internal standard. Multiplicities in parentheses are derived from off-resonance spectra. Long-range coupling constants (J_{CH}), which are not shown in Table 1, are as follows. For **2**: $^2J_{C(1)H(7)}$ = 1.8, $^2J_{C(2)H(3)}$ = 1.5, $^2J_{C(4)H(3)}$ = 6.8, $^2J_{C(4)H(5)}$ = 2.8, $^2J_{C(5)H(4)}$ = $^2J_{C(5)H(6)}$ = 2.2, $^2J_{C(7)H(6)}$ = 1.8, $^3J_{C(1)H(3)}$ =7.0, $^3J_{C(2)H(7)}$ = 4.9, $^3J_{C(2)H(CH3)}$ = 3.7, $^3J_{C(3)H(5)}$ = 11.2, $^3J_{C(4)H(6)}$ = 10.1, $^3J_{C(5)H(3)}$ = $^3J_{C(5)H(7)}$ = 9.6, $^3J_{C(6)H(4)}$ = 11.4, $^3J_{C(7)H(5)}$ = 9.2, $^4J_{C(1)H(5)}$ = 1.8, $^4J_{C(4)H(7)}$ = 2.8, $^4J_{C(7)H(3)}$ = 1.8. Hz. For **1**: $^2J_{C(6)H(5)}$ = $^2J_{C(6)H(7)}$ = 2.0, $^3J_{C(1)H(8)}$ = $^3J_{C(3)H(4)}$ = 11.6, $^3J_{C(3a)H(5)}$ = $^3J_{C(8a)H(7)}$ = 10.5, $^3J_{C(3a)H(8)}$ = $^3J_{C(8a)H(4)}$ = 9.2, $^3J_{C(4)H(6)}$ = $^3J_{C(8)H(6)}$ = 10.5, $^3J_{C(5)H(7)}$ = $^3J_{C(7)H(5)}$ = 10.5, $^3J_{C(6)H(4)}$ = $^3J_{C(6)H(8)}$ = 10.1, $^4J_{C(1)H(4)}$ = $^4J_{C(3)H(8)}$ = 5.9 Hz. [b]Small abundant triplet signals due to ^2H substitution.

Table 2. ^1H NMR (400 MHz) Spectral Data for (A) Substrates, (B) Key Reaction Intermediates, and (C) Product Azulenes[a]

(A) substrates (**2** and **2**-d_3)					
compd	H(3)	H(4)	H(5)	H(6)	H(7)
2	6.76 (ddd)	7.10 (dddd)	6.88 (dddd)	7.26 (dddd)	7.21 (ddd)
	$^3J_{3,4}$ 9.9	$^3J_{4,5}$ 10.7	$^3J_{5,6}$ 6.6	$^3J_{6,7}$ 12.1	
2-d_3	*b*	7.10 (brs)	*b*	7.25 (brs)	*b*

(B) key reaction intermediates (**6** and **6**-d_3)					
compd	H(4)	H(5)	H(6)	H(7)	H(8)
6	7.45 (dd)	7.41 (ddd)	7.06 (dddd)	7.29 (ddd)	7.15 (dd)
	$^3J_{4,5}$ 11.1	$^3J_{5,6}$ 7.9	$^3J_{6,7}$ 10.8	$^3J_{7,8}$ 9.7	
6-d_3	*b*	7.40 (brs)	*b*	7.27 (brs)	*b*

(C) product azulenes (**1** and **1**-d_3)				
compd	H(4,8)	H(5,7)	H(6)	NH_2
1	8.01 (dt)	7.70 (ddt)	7.62 (tt)	8.10 (br s)
	$^3J_{4,5}$ 10.1	$^3J_{5,6}$ 9.5	$^4J_{4,6}$ 0.9	$^5J_{4,7}$ 0.9
1-d_3	*b*	7.70 (brs)	*b*	8.10 (br s)

[a]^{13}C NMR and ^1H NMR charts are shown in Supplementary Figure S3. The numbering for hydrogens follows that for carbons in Scheme 3. Chemical shifts and selected coupling constants are in δ scale and Hz unit, respectively. Solvents used were $CDCl_3$, CD_3OD, and Me_2SO-d_6 for the substrates (**2** and **2**-d_3), key reaction intermediates (**6** and **6**-d_3), and product azulenes (**1** and **1**-d_3), respectively, with Me_4Si as the internal standard. A chemical shift, which is not shown in Table 2, is δ 3.95 (s, OCH_3) for **2**. Coupling constants, which are not shown in Table 2, are as follows. For **2** and **2**-d_3: $^4J_{3,5}$ 1.1, $^4J_{4,6}$ 1.1, $^4J_{5,7}$ 2.3, $J_{4,7}$ 0.8 Hz. For **6**: $^4J_{4,6}$ 2.1, $^4J_{5,7}$ 0.8, $^4J_{4,7}$ 0.8, $^4J_{6,8}$ 1.0 Hz. [b]Chemical shifts denote very small abundant signals due to ^2H substitution.

key intermediate **6** has three D atoms, and the nucleophilic addition was found to occur via path A.

Calculations of Reaction Paths and Discussion. The two-stage reactions in Scheme 3 were investigated by B3LYP calculations. Scheme 5 illustrates the model for them. The counterion Na^+ in NaOMe is indispensable to seek reaction paths. Without the two cations, two $HC(CN)_2^-$ species are repulsive to each other, which leads to their infinite separation during geometry optimizations.

After many attempts of searching potential surfaces of elementary processes, we obtained the reaction mechanism depicted in Scheme 6.

First Stage. Supplementary Figure S1-1 shows the reactant like complex composed of the substrate 2-methoxytropone (**2**),

dx.doi.org/10.1021/jo300693n | J. Org. Chem. 2012, 77, 5318−5330

Scheme 3. Key Intermediate and the Position of Three Deuteriums of the Substrate, Key Intermediate and Product in the Nozoe Azulene Synthesis[a]

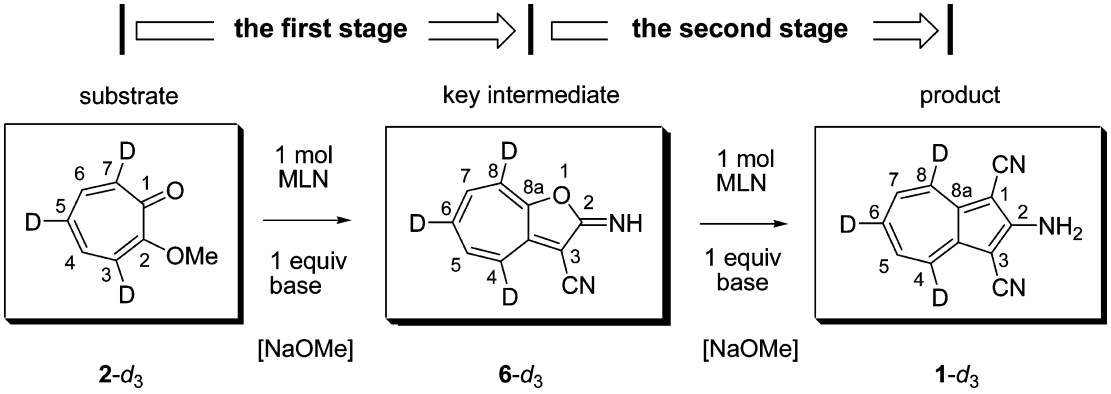

[a]MLN is malononitrile.

Table 3. ^{2}H NMR Spectra (61.4 MHz) for the ^{2}H-Labeled Substrate (2-d_3), Key Reaction Intermediate (6-d_3), and Product Azulene (1-d_3).[a]

compd	D(3)	D(5)	D(7)
2-d_3	1.59 (d, 1 D, J = 1.3 Hz)	1.71 (dd, 1 D, J = 1.8, 1.3 Hz)	2.05 (d, 1 D, J = 1.8)
compd	D(4)	D(6)	D(8)
6-d_3	4.12 (d, 1 D, J = 1.4 Hz)	3.76 (dd, 1 D, J = 1.4, 1.0 Hz)	3.82 (d, 1 D, J = 1.0 Hz)
compd	D(4,8)	D(6)	
1-d_3	4.63 (d, 2 D, J = 1.1 Hz)	4.04 (t, 1 D, J = 1.1 Hz)	

[a]The numbering for deuterium follows that for carbons in Scheme 3. Chemical shifts are presented in δ scale from the external standard, D_2O. Solvents used were $CHCl_3$, MeOH, and dioxane for 2-d_3, 6-d_3, and 1-d_3, respectively.

$(HCC_2N_2Na)_2$, and $(MeOH)_8$. MeOH molecules are linked to oxygen and nitrogen lone-pair orbitals as constructed in Scheme 5. Hereafter, bold numbers attached to structural formulas in Scheme 6 are commonly used to represent optimized geometries with the stoichiometry $C_{22}H_{42}N_4Na_2O_{10}$. From the precursor, a nucleophilic addition TS, TS(**2** → **3**), was obtained and is shown in Figure S1-2. The adduct **3** (Figure S1-3) is a Meisenheimer complex. From the complex, the MeO^- group is dissociated via TS(**3** → **4**) in Figure S1-4. After TS(**3** → **4**), a neutral intermediate, 2-troponylmalononitrile (**4**) in Figure S1-5, was afforded. The intermediate has an active methine group, which is subject to the deprotonation by MeO^- at TS(**4** → **5**) in Figure S1-6. The deprotonation led to the anion intermediate **5** shown in Figure S1-7. The anion **5** has seven canonical resonance structures and should be very stable. In **5**, the exocyclic oxygen atom is adjacent to the carbon atom in one cyano group. Here, a ring closure TS, TS(**5** → **6**) in Figure S1-8, was obtained successfully. Noteworthy is that the C(15)···O(2) ring closure is associated with the proton H(19) migration. The closure is caused by the enhancement of the electrophilicity of the cyano carbon by the proton attachment. After TS(**5** → **6**), the key intermediate **6** shown in Figure S1-9 is brought about. Thus, B3LYP calculations indicated that the first stage, **2** → **6** (see Scheme 6), consists of four consecutive elementary processes.

Second Stage. In the second stage, the key intermediate **6** is subject to the nucleophilic addition of the second $HC(CN)_2^-$ reagent. The addition sites may be predicted by the shape of the LUMO of **6**. Scheme 7 illustrates the shape and indicates that positions 4, 5, 6, 7, and 8a in the seven-membered ring are potentially targets of the $HC(CN)_2^-$ addition, and corresponding transition states were obtained.

The transition states are TS(**6** → **16**), TS(**6** → **17**), TS(**6** → **18**), and TS(**6** → **7**) (see Scheme 6), which are shown in Figure S2-1, S2-3, S2−5 and S2-7, respectively. Among the four adducts, **16** (Figure S2-2), **17** (Figure S2-4), and **18** (Figure S2-6) seem

Scheme 4. Path A (Normal) versus Path B (Abnormal) Nucleophilic Substitution

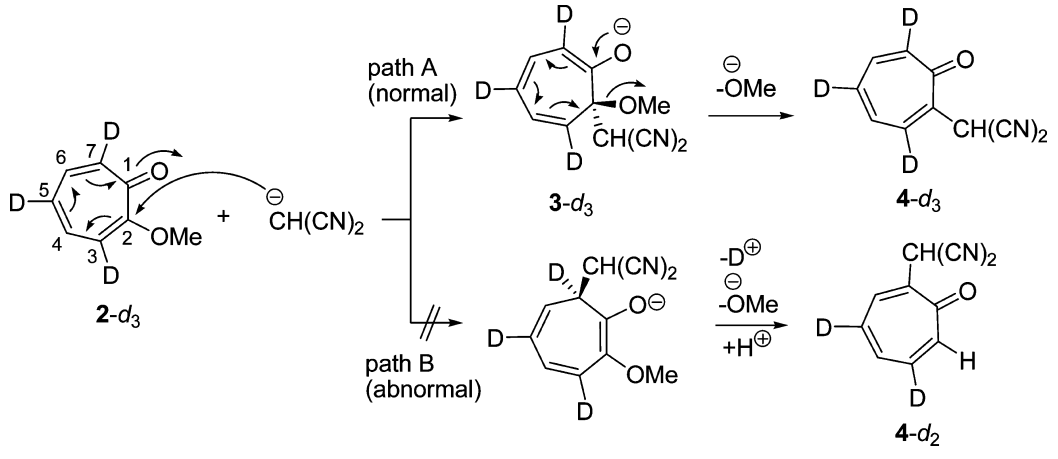

dx.doi.org/10.1021/jo300693n | J. Org. Chem. 2012, 77, 5318−5330

Scheme 5. Reaction Model Composed of 2, $(CH_3OH)_8$, and $[NaHC(CN)_2]_2$[a]

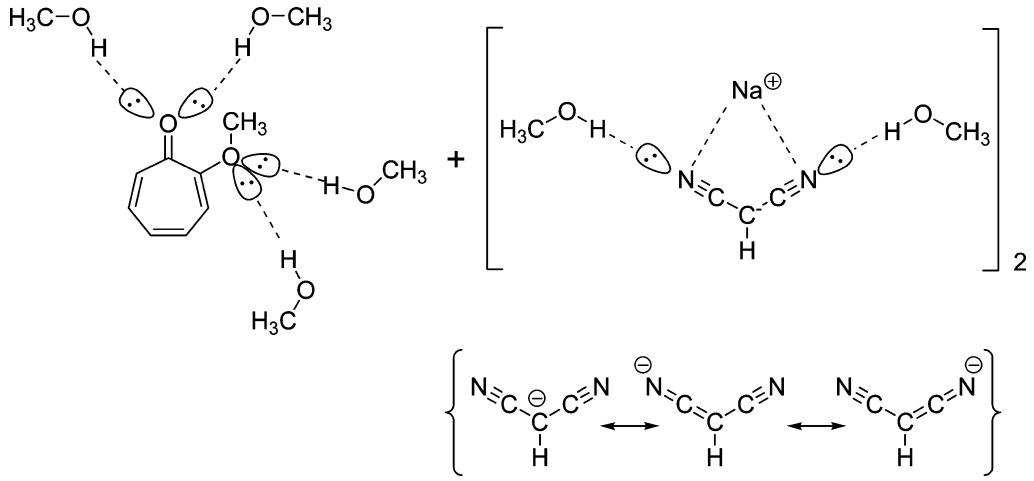

[a] $(CH_3OH)_2$ and Na^+ are coordinated to the $HC(CN)_2^-$ anion (with three canonical resonance formulas in curly braces).

not to have further channels toward the azulene product. However, these adducts and their neutralized species, ($\mathbf{16}H^+$), ($\mathbf{17}H^+$), and ($\mathbf{18}H^+$), might be trapped by careful detection.

Reaction paths starting from the adduct **7** (Figure S2-8 and Scheme 6) were searched for. Although **7** is an anion species, the hydrogen in the dicyanomethyl group is protonic enough to be eliminated. The elimination is expected by the presence of the strong base MeO^- formed at TS(**5** → **6**). The elimination TS, TS(**7** → **7a**), was obtained and is shown in Figure S2-9. The dianion species, **7a** (Figure S2-10), is unstable and undergoes protonation at the exocyclic imino nitrogen. The TS(**7a** → **8**) is shown in Figure S2-11. The protonation leads to a monoanion **8** shown in Figure S2-12. In the geometry of **8**, the C(1)−O(2) ether bond in the five-membered ring is long (1.532 Å), and its cleavage is likely. The ring scission TS, TS(**8** → **9**) is shown in Figure S2-13. The monocyclic intermediate **9** is yielded and is shown in Figure S2-14. In the monoanion **9**, the distance between C(14) and C(65) is 2.949 Å. Its linkage TS, TS(**9** → **10**), is shown in Figure S2-15. The ring formation is enhanced by the $Na(79)^+$ catalyst to N(11) for the electrophilicity of the C(65) atom in the cyano group. The ring formed intermediate, **10**, has the azulene skeleton and is shown in Figure S2-16. The exocyclic imino nitrogen is subject to the protonation at TS(**10** → **11**) exhibited in Figure S2-17. A neutral intermediate **11** is generated and is shown in Figure S2-18.

The neutral species **11** would undergo nucleophilic attack of MeO^-. One possible path is the addition−elimination or S_N2 on the carbonyl carbon of the amide group of **11** (Scheme 8). An S_N2 TS, TS(**11** → **12** + **13**), was obtained and is shown in Figure S2-19. After TS(**11** → **12** + **13**), the conjugate base of azulene (**12**) and methyl carbamate (H_2NCO_2Me, **13**) was obtained (Figure S2-20). Noteworthy is that the azulene anion **12** is the leaving group of S_N2. The other possible path is the elimination (E2 or E1cB) at the amide group of **11** (Scheme 8). One of the amino protons H(19) is taken off by the Me-O(38)$^-$ nucleophile at TS(**11** → **14**) shown in Figure S2-21. The resultant anion (E1cB intermediate) **14** is shown in Figure S2-22. From the anion **14**, the C(15)···C(14) bond is cleaved at TS(**14** → **12** + **15**) exhibited in Figure S2-23. Then, the conjugate base **12** and O═C═N$^-$ (cyanate ion) **15** via O═C═NH are formed, which are shown in Figure S2-24. The superiority or inferiority of S_N2 (Figure S2-19) and E1cB (Figures S2-21 and S2-23) TSs will be examined by the energy diagram.

Energy Changes of the First and Second Stages. First, the superiority or inferiority bewteen S_N2 and E1cB paths shown in Scheme 6 (from **11**) was examined. The activation energy of TS(**11** → **12** + **13**) (Figure S2-19) was computed to be +34.11 kcal/mol relative to the energy of **11**. On the other hand, that of TS(**14** → **12** + **15**) (Figure S2-23, the rate-determining step of E1cB) is 0.45 kcal/mol. Thus, the E1cB path is much more favorable than the S_N2 one, which is shown in Figure 1c. The entire energy diagram with the E1cB path is exhibited in Figure 1a.

Starting from the energy of **2** (Figure S1-1), its sharp descent toward that of **12** + **15** (Figure S2-24) was obtained. The exothermic descent demonstrates that the azulene formation is spontaneous and is of high reactivity. The rate-determining step is the nucleophlic addition of the first $HCC(CN)_2^-$ reagent to the substrate **2**, TS(**2** → **3**), of Figure S1-2. Noteworthy is that the energy of the anion **5** is more stable than that of the key intermediate **6**. The anion **5** might be detected in the salt form, **5**·Na^+. Also, some of three adducts **16**, **17**, and **18** (see Scheme 6) and/or their neutral species $\mathbf{16}H^+$, $\mathbf{17}H^+$ and $\mathbf{18}H^+$ might be detected. This is because the adduct **7** (toward the azulene) is most unstable among the four adducts, **16**, **17**, **18**, and **7** (Figure 1b). On the other hand, the activation free energies shown in Figure S2-1, S2-3, S2-5. and S2-7 indicate that formation of adducts **18** and **7** is unfavorable.

Experimental verification of the complicated reaction routes depicted in Scheme 6 is needed. Apparently, they are inconsistent with the simple conversion **2** → **6** → **1**, with the almost 100% yield shown in Scheme 3.

Experimental Challenge of Searching for Transient Reaction Intermediates. In Scheme 3, the reaction process **2** → **6** → **1** has been established. In the route **2** → **6** of the first stage, the furan ring fused to the seven-membered ring is formed. In the route **6** → **1** of the second stage, the furan ring is transformed to the carbocyclic five-membered ring of **1**. The reaction mechanism of Scheme 6 has been supported by DFT calculations. Intervention of various intermediates has been suggested by them. In order to examine the intervention, we attempted to isolate or detect them by low-temperature NMR spectroscopy. Parallel experiments with unlabeled and labeled substrates (**2** and **2**-d_3) and key intermediates (**6** and **6**-d_3) were conducted.

dx.doi.org/10.1021/jo300693n | J. Org. Chem. 2012, 77, 5318−5330

Scheme 6. Elementary Processes Obtained by B3LYP/6-31(+)G(d) Calculations[a]

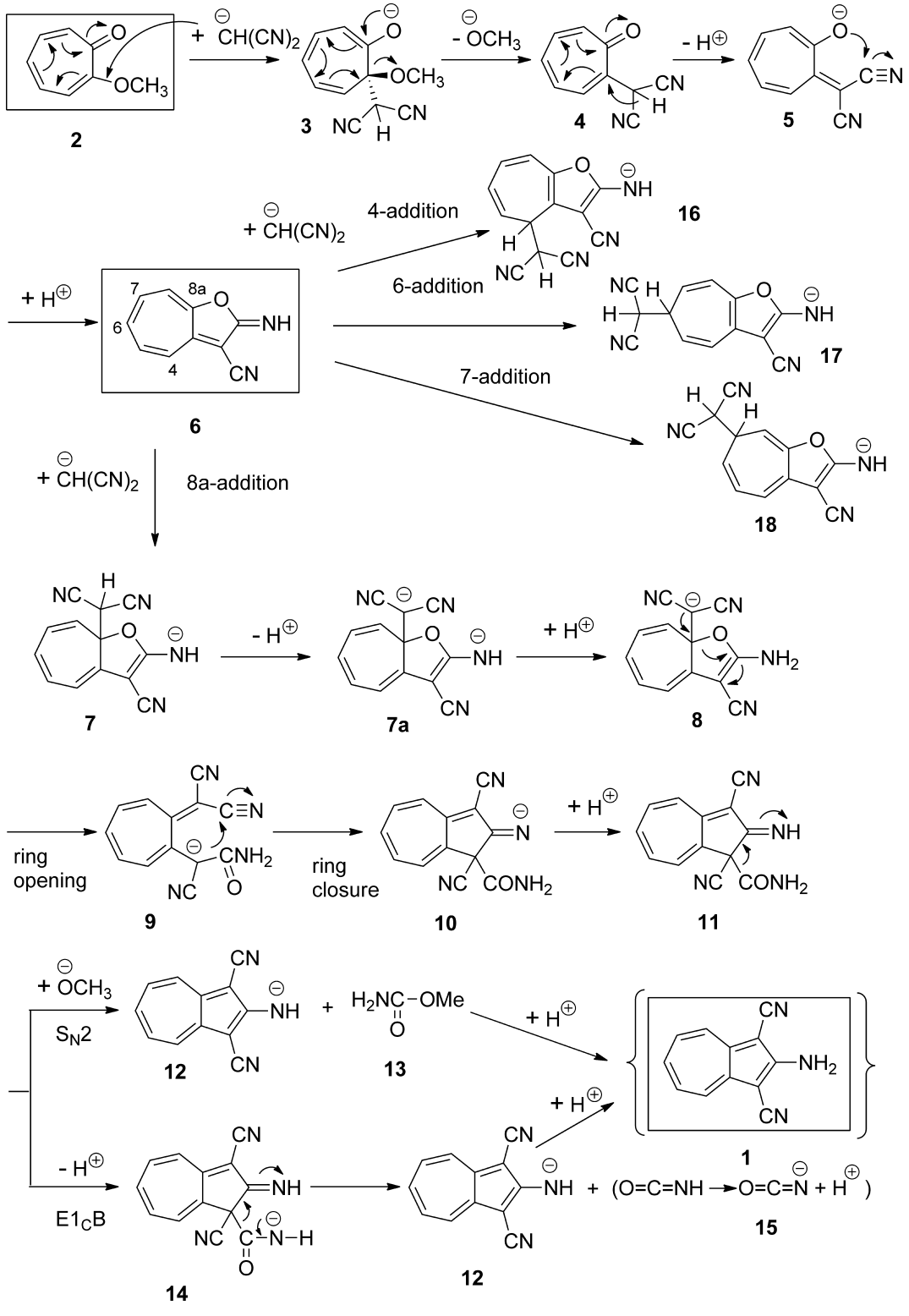

[a]The product azulene (**1**) is not included in the calculations, because it is formed by acidification of the solution containing the conjugated base **12**. Geometries of all intermediates and transition states are exhibited in Supplementary Figure S1 (the first stage, **1** → **6**) and Supplementary Figure S2 (the second stage, **6** → **12**).

The nearly monotonic and sharp energy stabilization toward the conjugate base of **1** (i.e., **12**) has been shown in Figure 1a by DFT calculations. There, the model includes [Na^+ and $HC(CN)_2^-$]$_2$ (Scheme 5). Then, to detect transient species, careful neutralization of the basic solution is needed. In particular, the deprotonation from the active methine group $(CN)_2HC$-H is quite ready and should be blocked against further reaction progress. Choosing experimental conditions precisely,

dx.doi.org/10.1021/jo300693n | J. Org. Chem. 2012, 77, 5318−5330

Scheme 7. LUMO Shape of the Key Intermediate 6 Calculated by the RHF/STO-3G Method; Orbital Coefficients of Respective Lobes Are Shown

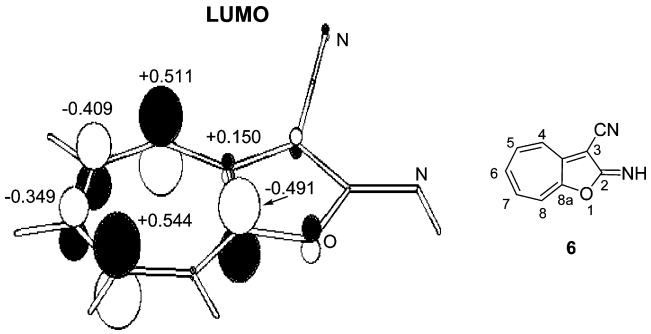

Scheme 8. Two Channels of Nucleophilic Reactions (S_N2 and E1cB), Where the Azulene Moiety Is the Leaving Group

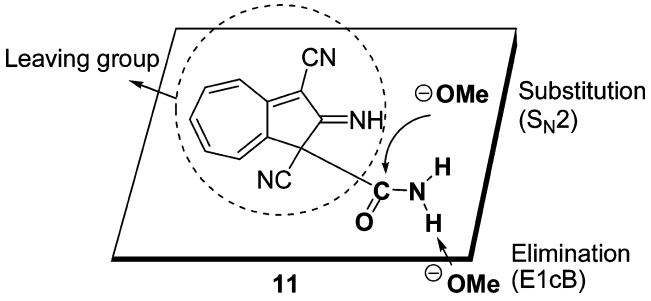

we succeeded in trapping important intermediates. In Table 4, detected intermediates are displayed along with **6** and **1**. Tables S1 and S2 exhibit ^{13}C and ^{1}H NMR data of intermediates, respectively.

In run (iv) of Table 4, the anion **5**[20] was obtained. Yellow needles of Na^+ **5** were isolated. Thus, as shown in the energy diagram of Figure 1, the product in the first stage is the anion **5** (Na^+ salt) rather than the key intermediate **6**. In runs (vii), (viii), and (ix), intermediates **3**, **4**, and **5** of the first stage were detected by NMR. The binary solvent system consisting of $(D_3C)_2SO$ and D_3C-OD was used, because in the single solvent D_3C-OD, the addition of MeO^- to the substrate (**2**) proceeds too rapidly for us to detect transient species by ^{1}H NMR spectroscopy. By use of the binary solvent, instantaneous formation of the Meisenheimer complex **3** was successfully observed as a mixture with **2** at 10 °C. The upfield shift of the resonance of **3** is in agreement with the anion structure. The complex **3** is rapidly converted to the 2-dicyanomethyltropone (**4**) at 5 °C. The intermediate **4** is converted to the anion **5** at 20 °C. The elementary processes of the first stage shown in Scheme 6 have been followed.

In runs (v), (vi), (x), and (xi) of the second stage, the adducts **16** and **17** were detected along with **7**. The ^{1}H NMR spectroscopy has proven that the three adducts (**7**, **16**, and **17**) have dicyanomethyl groups at C-8a, C-4, and C-6 positions of **6**, respectively (see Table S2 in Supporting Information and Scheme 6). ^{2}H-containing products support the structural assignments for the undeuteriated species. The adduct **18** (in Figure S2-6) was not detected. This result is in accord with the largest activation energy of TS(**6** → **18**) among those of TS(**6** → **7**), TS(**6** → **16**), TS(**6** → **17**), and TS(**6** → **18**) in Figure 1b. In these runs, main adducts are **16** and **17** rather than **7**, which are indicated in their energy level in Figure 1b. The neutralized adduct $7H^+$ could not be isolated, because the anion **7** proceeds instantaneously to the subsequent steps toward the azulene product. On the other hand, the two neutralized adducts, $16H^+$ and $17H^+$, could be successfully isolated as pale yellow crystals. They were obtained by careful preparative-thin-layer chromatography (PTLC) developed at low temperatures below −20 °C. When they are dissolved into methanol, they are decomposed to the key intermediate **6** and MLN. The half-life time of $16H^+$ was measured in MeOH to be $t_{1/2}$ = ca. 1 min at 25 °C and ca. 2 h at −40 °C. That of $17H^+$ is $t_{1/2}$ = ca. 2 min at 25 °C and ca. 4 h at −40 °C. Thus, the adducts **16** and **17** are merely equilibrating with **6** and do not contaminate the azulene formation. The **6** → **7** path, although less favorable than the **6** → **16** and **6** → **17** paths, is the sole nonequilibrium (irreversible) channel and gives the azulene according to the Le Chatelier's principle.

All of the results in Table 4 are consistent with DFT results aside from protonated (neutral) species such as $16H^+$ and $17H^+$.

Results of NMR measurements of intermediates predicted in Scheme 6 were reviewed. In the first stage (**2** → **6**), **3**, **4**, and **5** could be observed. In the second stage (**6** → **12**), **16**, **17**, **7**, **9**, and **11** were detected successfully along with protonated species $8H^+$ (same as $7H^+$), $9H^+$, $16H^+$, and $17H^+$. These are neutral intermediates equilibrating with their conjugated bases (the corresponding anions) and would stay in branch roads off the channel to the azulene. Intermediate species in the main road to the azulene are generally transient and difficult to observe. Those resting in branch roads are more detectable by NMR. As far as the reaction channel is concerned, the central skeleton should be anionic with resonance structures of the [7]annulenone ring and with avoidance of formation of the unstable methoxide ion (MeO^-). Exceptionally, the skeleton becomes neutral to undergo the subsequent nucleophilic attack.

■ CONCLUDING REMARKS

The Nozoe azulene-formation reaction is very useful to obtain 1,2- and 3-substituted azulenes. While the Hafner reaction in Scheme 1 involves formation of the seven-membered ring in the azulene, the Nozoe reaction involves that of the five-membered ring. This synthesis can be simply performed without any difficulty or catalysts, and the product yield is almost quantitative. In contrast to the synthetic utility, its reaction mechanism has been veiled for a long time, whereas the **2** → **6** → **1** process (Scheme 3) has been known. DFT calculations of a model reacting system composed of 2-methoxytropone (**2**), $[Na^+ HC(CN)_2^-]_2$,and $(MeOH)_8$ were carried out. While many elementary processes were found, the energy changes (Figure 1a) are of the spontaneous and high-reactivity reaction.

In order to assess the calculated result, precise experiments were conducted. First, more than 99.5% ^{2}H-labeled substrate, **2**-d_3, was prepared successfully. The purity led to the accurate measurement of the ^{2}H NMR (Table 3) and to the assignment of the unique reaction route toward the azulene product. By careful low-temperature experiments, anionic Meisenheimer adducts, **3**, **7**, **16**, and **17**, were detected spectroscopically by NMR. Furthermore, the salt intermediate (Na^+·**5**) and the neutralized adducts ($16H^+$ and $17H^+$) were isolated successfully. Despite the presence of these isolable intermediates, the azulene formation occurs quantitatively. The Nozoe reaction involves effective bond interchanges with negative-charge migrations through the [7]annulenone ring. The reaction seems to bear beautiful nucleophilic processes according to Le Chatelier's principle, which are shown in Scheme 9.

dx.doi.org/10.1021/jo300693n | J. Org. Chem. 2012, 77, 5318−5330

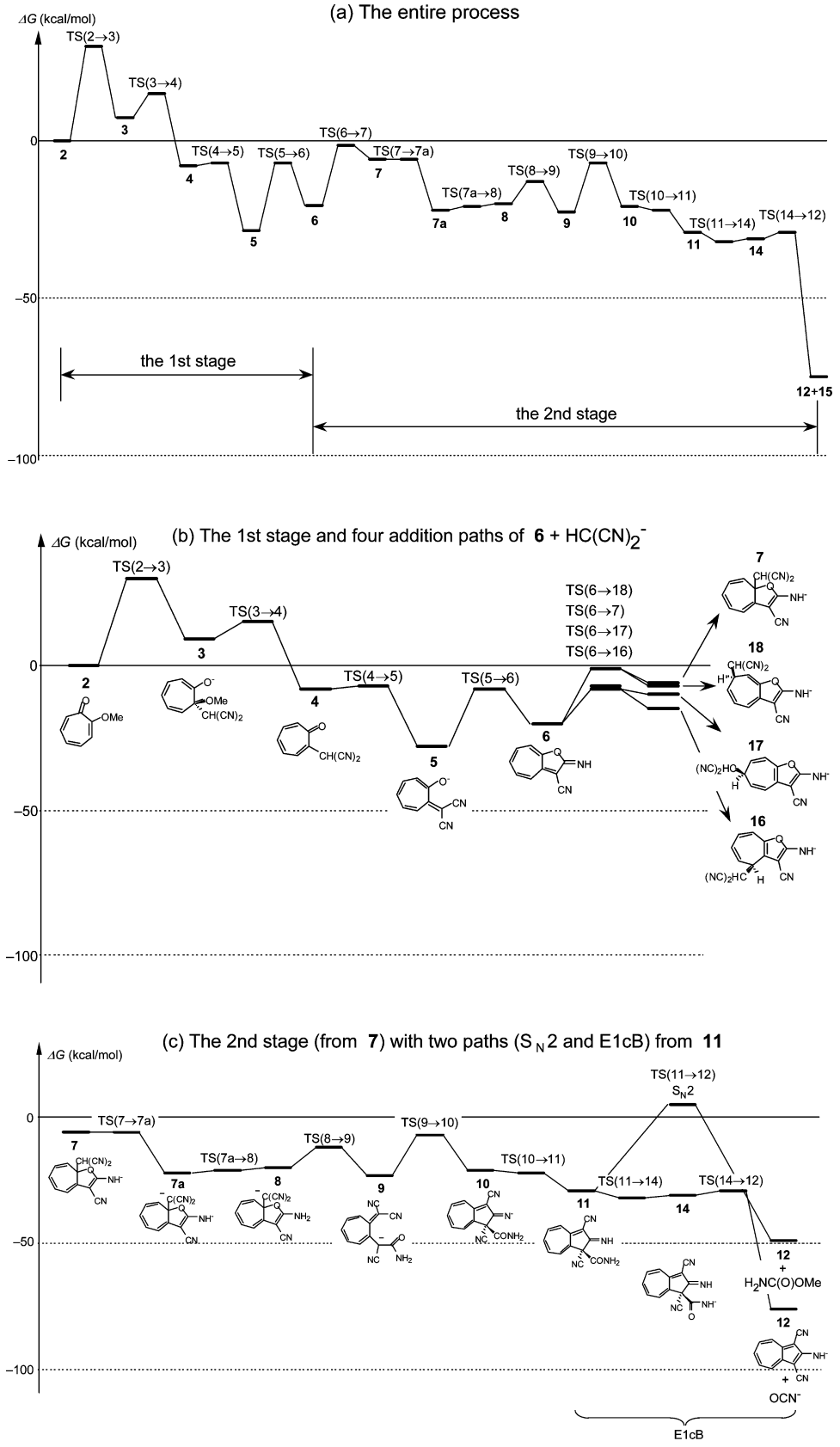

Figure 1. Changes of Gibbs free energies (T = 298.15 K, P = 1 atm) calculated by B3LYP/6-311+G(d,p) [SCRF = PCM, solvent = methanol]//B3LYP/6-31(+)G(d) thermal correction. Their values are shown in the captions of Supplementary Figures S1−1 through S1−9 and S2−1 through S-24 of Supporting Information. Panel (a) shows the energy profile of the entire process, and panels (b) and (c) show its components with competitive paths from **6** (b) and **11** (c). Free energies were evaluated by a splicing method (the sum of single-point electronic energies and thermal corrections). Therefore, some TS energies are slightly smaller than intermediate ones.

dx.doi.org/10.1021/jo300693n | J. Org. Chem. 2012, 77, 5318−5330

Table 4. Parallel Experiments (without and with 3,5,7-$^2H_3$ Labeled Species) To Detect and Trap Transient Intermediates[a]

run	reaction	condition and result	isolated yield (%)
		Azulene Formations in Schemes 2 and 3	
(i)	**2** → **1** (**2**-d_3 → **1**-d_3)	MLN (2 equiv), NaOMe (2 equiv), MeOH, room temperature, 12 h	96−99
(ii)	**6** → **1** (**6**-d_3 → **1**-d_3)	MLN (1 equiv), NaOMe (1 equiv), MeOH, room temperature, 6 h	98−100
		For the Isolation of the Reaction Intermediates	
(iii)	**2** → **6** (**2**-d_3 → **6**-d_3)	MLN (1 equiv), NaOMe (1 equiv), MeOH, 20 °C, 12 h, neutralization with dil HCl	92
(iv)	**2** → **5** (**2**-d_3 → **5**-d_3)	MLN (1 equiv), NaOMe (1 equiv), MeOH, 20 °C, 12 h	97−98
(v)	**6** → **16** (**6**-d_3 → **16**-d_3)	MLN (1 equiv), MeOH, 0 °C, 2 h, maximum concentration, 52% by NMR[b]	
	→ **16**H$^+$ (→ **16**H$^+$-d_3)	separated on PTLC [SiO_2, CH_2Cl_2−ether (1:1), −20 °C]	37−50
(vi)	**6** → **17** (**6**-d_3 → **17**-d_3)	MLN (1 equiv), MeOH, −20 °C, 30 min, maximum concentration, 67% by NMR[b]	
	→ **17**H$^+$ (→ **17**H$^+$-d_3)	separated on PTLC [SiO_2, CH_2Cl_2−ether (1:1), −20 °C]	41
		For the NMR-Spectroscopic Detection of the Transient Reaction Intermediates[c]	
(vii)	**2** → **3** (**2**-d_3 → **3**-d_3)	MLN (1 equiv), $NaOCD_3$ (1 equiv), Me_2SO-d_6−CD_3OD (9:1), 5 °C, instantaneously (0 min.) NMR detected[b]	
(viii)	**2** → **4** (**2**-d_3 → **4**-d_3)	MLN (1 equiv), $NaOCD_3$ (1 equiv), Me_2SO-d_6−CD_3OD (9:1), 5 °C, 30 min, NMR detected[b]	
(ix)	**4** → **5** (**4**-d_3 → **5**-d_3)	$NaOCD_3$ (1 equiv), Me_2SO-d_6−CD_3OD (9:1), 20 °C, 5 h, NMR detected	
(x)	**6** → **7** + **16** (**6**-d_3 → **7**-d_3 + **16**-d_3)	MLN (1 equiv), $NaOCD_3$ (1 equiv), CD_3OD, −50 °C, instantaneously, NMR detected[b]	
(xi)	**6** → **16** + **17** (**6**-d_3 → **16**-d_3 + **17**-d_3)	MLN (1 equiv), $NaOCD_3$ (1 equiv), CD_3OD, −20 °C, instantaneously, NMR detected[b]	
(xii)	**6** → **8**H$^+$ (**6**-d_3 → **8**H$^+$-d_3)	MLN (1 equiv), CD_3OD, −50 °C, 30 min, maximum concentration, 32% by NMR[b]	
(xiii)	**6** → **9**H$^+$ (**6**-d_3 → **9**H$^+$-d_3)	CD_3OD, 0 °C, 1 h, maximum concentration 31% by NMR[b]	
(xiv)	**6** → **9** (**6**-d_3 → **9**-d_3)	MLN (1 equiv), $NaOCD_3$ (1 equiv), CD_3OD, 0 °C, instantaneously, maximum concentration, 2% by NMR[b]	
(xv)	**9** → **11** (**9**-d_3 → **11**-d_3)	CD_3OD, 20 °C, 8 h, maximum concentration, 44% by NMR[b]	

[a]MLN is malononitrile, $H_2C(CN)_2$. Numbered species in the "reaction" columns are shown in Scheme 6. Structural formulas of d_3-species except **1**-d_3, **2**-d_3, and **6**-d_3 (Scheme 3):

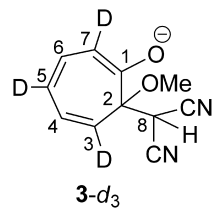

3-d_3

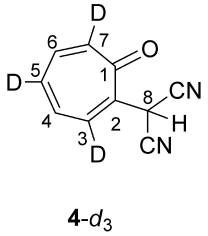

4-d_3

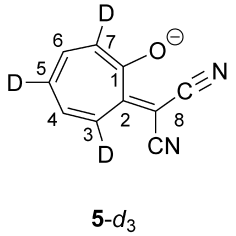

5-d_3

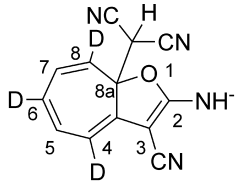

7-d_3

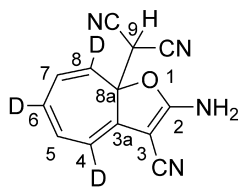

8H$^+$-d_3

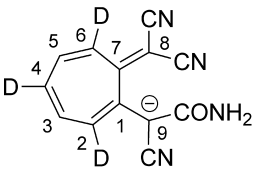

9-d_3

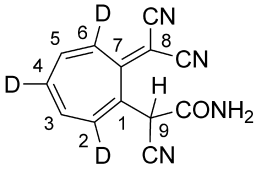

9H$^+$-d_3

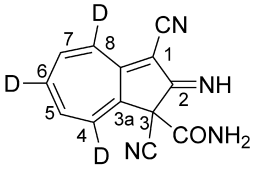

11-d_3

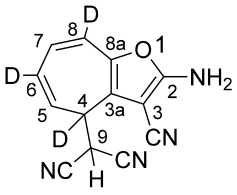

16H$^+$-d_3

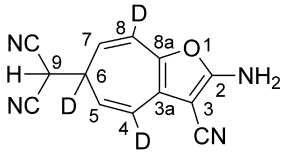

17H$^+$-d_3

[b]NMR spectra at low temperature are shown in Figure S3 of the Supporting Information. [c]Neutral species **8**H$^+$ and **9**H$^+$ are formed by proton transfers, **8** + MeOH → **8**H$^+$ + MeO$^-$ and **9** + MeOH → **9**H$^+$ + MeO$^-$, respectively. Those species are thought to merely intervene by equilibration in byways not concerned with the route to azulene product.

EXPERIMENTAL SECTION

Reagents, Starting Material, and Manipulation. The starting material, tropolone (**19**), was prepared from tropone[21] via 2-aminotropone by a literature method.[22] The undeuteriated substrate, 2-methoxytropone[23] (**2**), was prepared from **19** according to a literature method. In a similar way, the deuteriated substrate, 2-methoxy-[3,5,7-$^2H_3$]tropone (**2**-d_3), was synthesized from [3,5,7-$^2H_3$]tropolone (**19**-d_3) and diazomethane (H_2CN_2). To obtain high isotopic purity (>99%) of **19**-d_3 the deuteriation process was repeated three times. The methanol solvent used was spectro-grade and was dried over 3 Å molecular sieves. Deuterium oxide (isotopic purity 99.97%) was used for deuterium labeling experiments. For PTLC, silica gel (0.063−0.200 mm) was employed. Samplings for all of the NMR monitoring experiments were performed using high-vacuum line (<10^{-4} Torr) techniques and were degassed by three successive freezing−pump−thaw cycles to 10^{-4} mmHg. NMR tubes for sealed tube experiments were flame-dried under vacuum immediately prior to the experiments. Low-temperature chromatographies were carried out in a cooling globe box under nitrogen stream.

Instrumentation/Analytical Procedures. Melting points were determined in open capillary tubes and are uncorrected. IR spectra were recorded using KBr disks unless otherwise noted. UV−vis spectra were taken in methanol. Electron impact (EI) mass spectra (MS) as well as fast atom bombardment (FAB) MS were obtained at 70 eV. The values of m/z in significant ions are reported with relative intensities in parentheses (percent for the base peak) for low resolution analyses. NMR (^{13}C, ^1H, and ^{17}O) spectra were recorded in $CDCl_3$ at 100.6, 400, 61.4, and 54.2 MHz for ^{13}C, ^1H, ^2H, and ^{17}O nuclei, respectively, unless otherwise specified, with Me_4Si (for ^{13}C and ^1H) or D_2O (for ^2H and ^{17}O) as the standard.

dx.doi.org/10.1021/jo300693n | J. Org. Chem. 2012, 77, 5318−5330

Scheme 9. Summary of the Present Results[a]

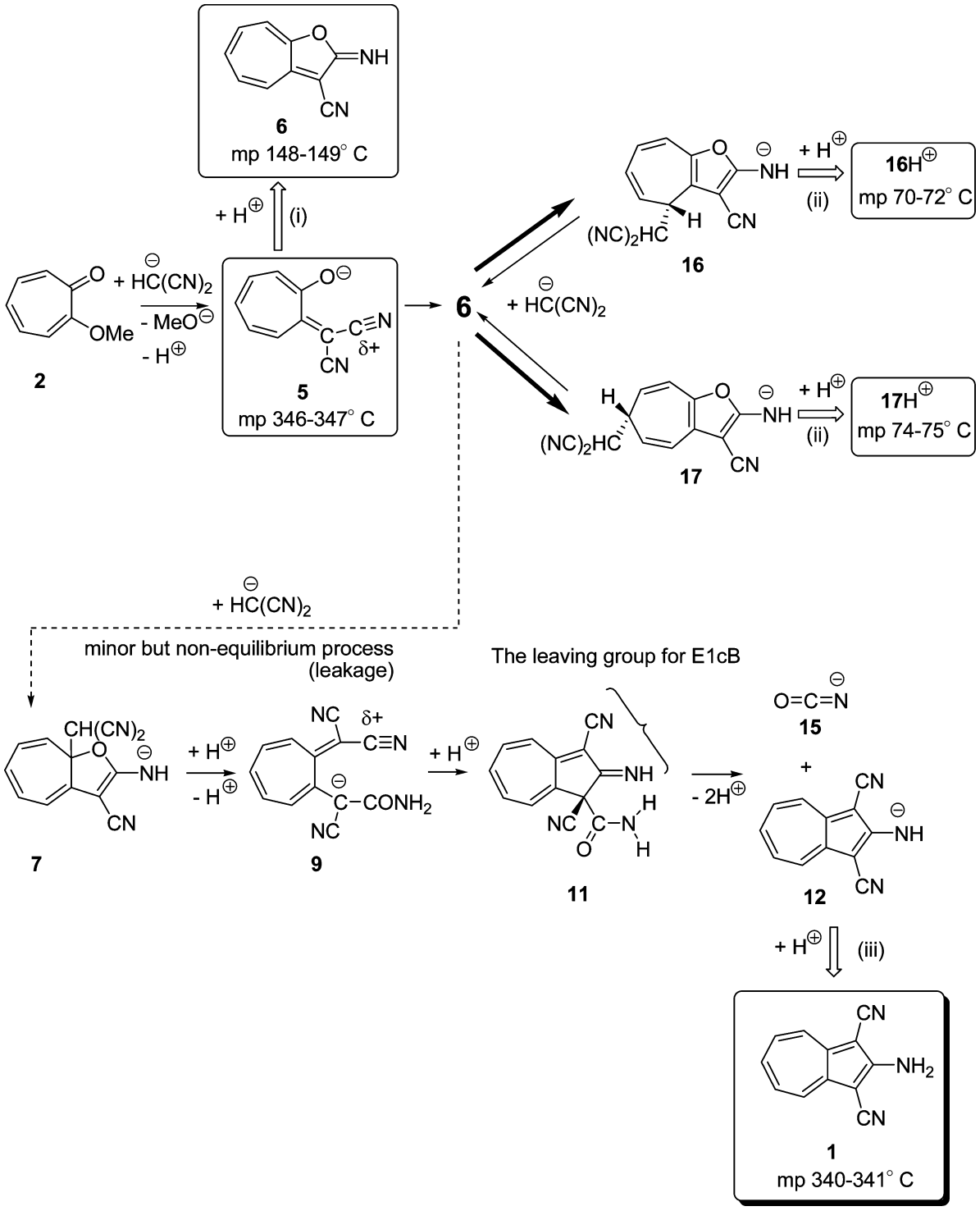

[a]Species in boxes are the isolated ones with melting points. Bold empty arrows (i), (ii), and (iii) indicate neutralization processes. Anions **5** and **9** are precursors for the ring closures. The azulene **1** is the final product of the second stage with almost 100% yield when interruptions (i.e., neutralizations (i) and (ii)) are absent.

Preparation of [3,5,7-$^2H_3$]Tropolone (19-d_3). A sealed tube containing 12.20 g of tropolone and 60 mL of D_2O (isotopic purity, ca. 96%) was heated at 200 °C for 16 h. This procedure was repeated three times using D_2O with the high isotopic purity (99.97%). The resulted mixture was extracted with anhydrous ether. The water layer was further extracted continuously with ether overnight. Solvent removal left 11.57 g of pale brownish solid, which was dissolved in wet ether and stirred for 2 h. The solution was dried over $MgSO_4$. Solvent removal followed by sublimation at 90 °C (5−7 mmHg) gave 11.50 g (92%) of **19**-d_3 as colorless needles. The mixed mp was not depressed with an authentic sample of an undeuteriated sample: colorless needles, mp 50−51 °C (sublimation); isotopic purity, 99.6% $^2H_3$; 0.4% $^2H_2$, from mass spectrometry; IR ν_{max} 3520, 3224, 1608, 1554, 1480, 1268, 744, 662 cm^{-1}; ^{1}H NMR δ 9.21 (brs, 1 H, OH), 7.40 (brs, 2 H, H-4,6), 7.36 (very small abundant d, $^3J_{H(3)-H(4)}$ = 9.7 Hz, H-3,7), 7.05 (very small abundant t, $^3J_{H(4)-H(5)}$ = 9.6 Hz, H-5); ^{13}C NMR δ 123.62 (small abundant t, $^1J_{C-D}$

dx.doi.org/10.1021/jo300693n | J. Org. Chem. 2012, 77, 5318−5330

= 23.9 Hz, C-3,7), 127.94 (small abundant t, $^1J_{C-D}$ = 22.7 Hz, C-5), 137.49 (d, C-4,6), 171.99 (s, C-1,2); MS *m*/*z* 125 (M^+, 100), 97 (65), 69 (49), 68 (27).

Preparation of 2-Methoxy[3,5,7-$^2H_3$]tropone (2-d_3). To a stirred solution of 6.25 g (50 mmol) of [3,5,7-$^2H_3$]tropolone (**19**-d_3) in 250 mL of ether was added dropwise freshly distilled ethereal solution (150 mL, 0.12 mol) of diazomethane. The solution was stirred at 25 °C for 2 h, until the complete consumption of **19**-d_3 in the solution was detected [no indication of the violet color by a test with ferric(III) chloride solution]. Workup followed by Kugelrohr distillation gave 6.67 g (96%) of pure **2**-d_3 (isotopic purity, d_3, 99.6%; d_2, 0.4%, by mass spectrometry): pale yellow oil, bp 124−125 °C (2.0 Torr) [lit.[15] bp 90 °C (3 Torr)]; IR (neat) ν_{max} 1614, 1582, 1174, 742, 672 cm^{-1}; MS *m*/*z* 139 (M^+, 47), 111 (33), 110 (35), 108 (76), 96 (12), 81 (83), 80 (37), 68 (100).

Procedure for Azulene Synthesis Using 2-Methoxytropone (2) and Malononitrile (MLN) in the Presence of 2 mol of Sodium Methoxide. In a typical case, to a suspension of the sodium salt of MLN [prepared from 460 mg (20 mmol) of metallic sodium and 20 mmol of MLN] in 20 mL of methanol was added dropwise a solution of 10 mmol of 2-methoxytropone (**2**, 1.36 g) or 2-methoxy[3,5,7-$^2H_3$]tropone (**2**-d_3, 1.39 g) in 10 mL of methanol at 0 °C. The reaction mixture was stirred at room temperature overnight. The precipitate that separated out was collected by filtration and was washed with water and ethanol to give crystals of 2-amino-1,3-dicyanoazulene **1** (1.91 g, 99%) or 2-amino-1,3-dicyano[4,6,8-$^2H_3$]azulene **1**-d_3 (1.88 g, 96%). Spectral samples were obtained by recrystallization from acetone.

1: orange prisms, mp 340−341 °C in a sealed tube (lit.[14g] mp 305 °C); sublimative at 265 °C; IR ν_{max} 3347, 3212, 2208, 1671, 1553, 1538, 1514, 742, 702 cm^{-1}; UV−vis λ_{max} 231 (log ε 4.50), 308 (4.66), 320 (4.71), 392 nm (3.84); MS *m*/*z* 193 (M^+, 100), 166 (23), 165 (28), 140 (14), 139 (33), 113 (12), 89 (14), 76 (22).

1-d_3: orange prisms, mp 341−341.5 °C; isotopic purity: d_3, 99.6; d_2, 0.4% (by mass spectrometry); IR ν_{max} 3368, 3231, 2211, 1673, 1556, 1511, 711, 656, 568 cm^{-1}; UV−vis λ_{max} 231 (log ε 4.53), 308 (4.70), 320 (4.75), 392 nm (3.87); MS *m*/*z* 196 (M^+, 100), 168 (33), 142 (31), 116 (12), 92 (22), 78 (17).

Procedure for the Isolation of an Intermediate, Sodium Salt 5. In a typical case, to a solution of 5 mmol of 2-methoxytropone (**2**, 1.36 g) in 10 mL of methanol was added dropwise a solution of sodium salt of MLN (670 mg, 10 mmol) in 23 mL of methanol at −30 °C. The reaction mixture was stirred for 1 h. The precipitate that separated out was collected by filtration and was washed with ether giving **5** (2.04 g, 98%). Analytical samples were obtained by recrystallization from cold ether−ethanol. **5**-d_3 (613 mg, 97%) was obtained from **2**-d_3 (450 mg) and the sodium salt of MLN (220 mg).

5: yellow needles, mp 346−347 °C (dec); IR ν_{max} 2211, 2171, 1595, 1528, 1458, 1421, 748, 705 cm^{-1}; UV−vis λ_{max} 238 (log ε 4.22), 263 (4.18), 402 (4.25), 417 nm (4.25); ^{17}O NMR (MeOH, D_2O) δ 377.61; FAB-MS *m*/*z* 193 (MH^+). Anal. Calcd for $C_{10}H_5N_2ONa$: C, 62.51; H, 2.62; N, 14.58. Found: C, 62.43; H, 2.55; N, 14.62.

5-d_3: yellow needles, mp 343−344 °C (dec); IR ν_{max} 2211, 2170, 1585, 1497, 1438, 734, 700 cm^{-1}; UV−vis λ_{max} 237 (log ε 4.21), 264 (4.18), 402 (4.24), 417 nm (4.24); FAB-MS *m*/*z* 196 (MH^+).

Procedure for the Isolation of Sodium-Free Intermediate, 2-Imino-2*H*-cyclohepta[*b*]furan-3-carbonitrile (6). To a mixture of MLN (66 mg, 10 mmol) and NaOMe (54 mg, 10 mmol) in 23 mL of methanol was added dropwise a solution of 1.36 g (10 mmol) of 2-methoxytropone (**2**) in 10 mL of methanol at 0 °C. The reaction mixture was stirred at room temperature for 12 h. Workup with dilute hydrochloric acid gave the product **6** (1.63 g, 94%). Extraction with dichloromethane followed by solvent removal gave **6** (1.56 g, 92%). Spectral samples were obtained by further recrystallization from cold acetonitrile. **6**-d_3 (1.59 g, 92%) was obtained from **2**-d_3 (1.39 g) and Na^+ $HC(CN)_2^-$ (66 mg).

6: orange prisms, mp 148−149 °C (dec) (lit.[14g] mp 143 °C); IR ν_{max} 3281, 2203, 1670, 1489, 1095, 750 cm^{-1}; UV−vis λ_{max} (MeOH) 208 (log ε 4.13), 238 (4.21), 262 (4.14), 403 (4.19), 417 (4.20); MS *m*/*z* 170 (M^+, 78), 143 (30), 116 (65), 88 (34), 58 (100). Anal. Calcd for $C_{10}H_6N_2O$: C, 70.58; H, 3.55; N, 16.46. Found: C, 70.46; H, 3.45; N, 16.22.

6-d_3: orange prisms, mp 145−146 °C (dec); isotopic purity: d_3, 99.3, d_2, 0.7% (by mass spectrometry); IR ν_{max} 3296, 2220, 1684, 1502, 1104, 752, 630 cm^{-1}; MS *m*/*z* 173 (M+, 100), 145 (36), 119 (66), 91 (31).

Procedure for the Reaction of 2-Imino-2*H*-cyclohepta[*b*]-furan-3-carbonitrile (6) with 1 mol of MLN To Give 2-Amino-1,3-dicyanoazulene (1) in the Presence of 1 mol of Sodium Methoxide. In a typical case, to a mixture of MLN (660 mg, 10 mmol) and NaOMe (10 mmol) in 23 mL of methanol was added dropwise a solution of **6** (1.70 g, 10 mmol) in 10 mL of methanol. The reaction mixture was stirred at room temperature overnight. The orange precipitate that separated out was collected by filtration and was washed with water. Recrystallization from acetone gave the azulene **1** (1.93 g, 100%) quantitatively. **1**-d_3 (544 mg, 100%) was obtained from **6**-d_3(480 mg) and MLN (183 mg).

Reaction of 2-Imino-2*H*-cyclohepta[*b*]furan-3-carbonitrile (6) with 1 mol of MLN without a Base: Isolation of Protonated Meisenheimer-Type Adducts (16H$^+$ and 17H$^+$). A mixture of **6** (850 mg) and MLN (33 mg) in methanol was stirred. In a rapid succession, solvent was removed under reduced pressure below −20 °C to leave viscous oil. The residue was separated into several components by PTLC [silica gel, dichloromethane−ether (9:1)] developed at −20 °C in a cool box. The desired component **16**H$^+$ or **17**H$^+$ was collected and recrystallized from cold ether or acetone. The spectral samples were further recrystallized from cold acetone. (a) Isolation of protonated intermediate **16**H$^+$: After the reaction was performed at −20 °C for 1 h, the desired component **16**H$^+$ (R_f 0.610, 436 mg, 37%) was separated by PTLC at −20 °C. The isolation of **16**H$^+$-d_3 was made similarly using **6**-d_3 in 50% yield. (b) Isolation of protonated intermediate **17**H$^+$: After the reaction was performed at 0 °C for 30 min, the desired component **17**H$^+$ (R_f 0.613, 430 mg, 41%) was isolated. The isolation of **17**H$^+$-d_3 was similarly done using **6**-d_3.

16H$^+$: yellow crystals, mp 70−72 °C, $t_{1/2}^{-40\ °C}$(MeOH) 2 h, $t_{1/2}^{25\ °C}$(MeOH) 1.2 min; IR ν_{max} 3444, 3348, 2216, 1652, 706 cm^{-1}; UV−vis λ_{max} (MeOH, −20 °C) 263 (log ε 4.03), 366 nm (3.80); MS (70 eV) *m*/*z* 236 (M^+, 5%), 170 (34), 66 (100). Anal. Calcd for $C_{13}H_8ON_4$: C, 66.10; H, 3.41; N, 23.72. Found: C, 66.23; H, 3.38; N, 23.82.

16H$^+$-d_3: yellow crystals, mp 70−72 °C; IR ν_{max} 3440, 3318, 2216, 1652, 706 cm^{-1}; UV−vis λ_{max} (EtOH, −20 °C) 263 (log ε 4.03), 366 nm (3.80); MS (75 eV) *m*/*z* 239 (M^+, 6%).

17H$^+$: pale yellow prisms, mp 74−75 °C, $t_{1/2}^{-40\ °C}$(MeOH) 4 h, $t_{1/2}^{25\ °C}$(MeOH) 2 min; IR (KBr) ν_{max} 3055 (w), 3040 (w) cm^{-1}; UV−vis λ_{max} (MeOH, 0 °C) 234 (log ε 4.04), 308 (3.76), 320 nm (3.82); MS *m*/*z* 221 (M + 1, 11%), 220 (M^+, 62%), 219 (22), 39 (23). Anal. Calcd for $C_{13}H_8ON_4$: C, 66.10; H, 3.41; N, 23.72. Found: C, 66.18; H, 3.35; N, 23.87.

17H$^+$-d_3: colorless prisms, mp 74−75 °C; IR (KBr) ν_{max} 3055 (w), 3040 (w) cm^{-1}; MS *m*/*z* 224 (M + 1, 11%), 223 (M^+, 62%), 222 (22), 42 (23).

Low-Temperature NMR (^1H and ^{13}C) Spectroscopic Detection of Unisolable Reaction Intermediates. Reaction monitoring was performed periodically. The analytical results for chemical shifts and coupling constants are listed in Tables S1−S2. Representatitve examples of the charts are exhibited in Figure S3. The ^{13}C NMR measurements were performed at a probe temperature of −90 °C.

Computational Methods Used. The reacting systems shown in Figures S1 and S2 were investigated by density functional theory calculations. The B3LYP method[24] was used. B3LYP seems to be a suitable method, because it includes the electron correlation effect to some extent. For the MeO^- containing reactions, the basis set employed was 6-31(+)G(d), where the diffuse functions denoted by (+) are added to the oxygen and nitrogen 6-31G(d). Since the present systems are large, calculations by the higher-level basis set are too difficult to trace reaction paths. Geometry optimizations were carried out by the RB3LYP/6-31(+)G(d) method. Transition states (TSs) were sought first by partial optimizations at bond interchange regions. Second, by the use of Hessian matrices, TS geometries were optimized and were characterized by vibrational analyses, which checked whether the

dx.doi.org/10.1021/jo300693n | J. Org. Chem. 2012, 77, 5318−5330

obtained geometries had single imaginary frequencies ($\nu^{\ddagger}$). From TSs, reaction paths were traced by the intrinsic reaction coordinate method[25] to obtain the energy-minimum geometries. Relative free energies ΔG were obtained by single-point calculations of RB3LYP/6-311+G(d,p) [self-consistent reaction field (SCRF) = PCM,[26] solvent = methanol] on the RB3LYP/6-31(+)G(d) electronic and thermal correction ones. All the calculations were carried out by the use of Gaussian 03[27] installed on computers of the Research Center for Computational Science, Okazaki Japan.

■ ASSOCIATED CONTENT

Supporting Information

Geometries obtained by B3LYP/6-31(+)G(d) optimizations in the first stage, **2** → **6**, and in the second stage, **6** → **12**; ^{1}H NMR and ^{13}C NMR data of the substrates, products, and intermediates; and Cartesian coordinates of the optimized geometries in Figures S1 and S2. This material is available free of charge via the Internet at http://pubs.acs.org.

■ AUTHOR INFORMATION

Corresponding Author

*E-mail: minatot@daibutsu.nara-u.ac.jp.

Notes

The authors declare no competing financial interest.

■ ACKNOWLEDGMENTS

Tetsuo Nozoe, Professor Emeritus of Tohoku University, passed away on April 4, 1996, one month before his 94th birthday. This is the last paper in his life-long career studying novel (non-benzenoid) aromatic chemistry. For his biography, see ref 7. The authors thank Ms. Ayaka Yamada for her partial assistance in DFT calculations.

■ REFERENCES

(1) For reviews, see: (a) Zeller, K.-P. Azulenes. In *Carbocyclische π-Elektronen-Systeme: Houben-Weyl, Methoden der organischen Chemie*; Müller, E., Bayer, O., Eds.; Georg Thieme: Stuttgart, Germany, 1985; Vol. *5/2c*, pp 127−419. (b) Nozoe, T. *Pure Appl. Chem.* **1972**, *28*, 239−280.

(2) (a) Minkin, V. I.; Glukhovtsev, M. N.; Simkin, B. Y. *Aromaticity and Antiaromaticity. Electronic and Structural Aspects*; Wiley: New York, NY, 1994. (b) Lloyd, D. *The Chemistry of Conjugated Cyclic Compounds*; Wiely: New York, NY, 1990. (c) Lloyd, D. *Non-benzenoid Conjugated Carbocyclic Compounds*; Elsevier: Amsterdam, 1984. (d) Garratt, P. J. *Aromaticity*; McGraw-Hill: New York, 1971.

(3) These unusual hydrocarbons have beautiful colors of blue, violet, or green and characteristic basicity.

(4) (a) Pfau, A. S.; Plattner, P. A. *Helv. Chem. Acta* **1936**, *19*, 858−879. (b) Plattner, P. A.; Pfau, A. S. *Helv. Chem. Acta* **1937**, *20*, 224−232.

(5) (a) Scott, L. T.; Roseboom, M. D.; Houk, K. T.; Fukunaga, T.; Lindner, H. J.; Hafner, K. *J. Am. Chem. Soc.* **1980**, *102*, 5169−5176. (b) Scott, L. T. *Pure Appl. Chem.* **1983**, *55*, 363−368. (c) Scott, L. T.; Grutter, P.; Chamberlain, R. E. *J. Am. Chem. Soc.* **1984**, *106*, 4852−4856. (d) Scott, L. T.; Adams, C. M. *J. Am. Chem. Soc.* **1984**, *106*, 4857−4861.

(6) (a) Nozoe, T.; Wakabayashi, H.; Shindo, K.; Kurihara, T.; Ishikawa, S.; Kageyama, M. *Chem. Lett.* **1995**, 25−26. (b) Takeshita, H.; Yan, Y. Z.; Kato, N.; Mori, A.; Nozoe, T. *Tetrahedron Lett.* **1995**, *36*, 5195−5198. (c) Takeshita, H.; Yan, Y. Z.; Kato, N.; Mori, A.; Wakabayashi, H.; Nozoe, T. *Tetrahedron Lett.* **1995**, *36*, 5199−5202. (d) Nozoe, T.; Takeshita, H. *Bull. Chem. Soc. Jpn.* **1996**, *69*, 1149−1178 and references therein.

(7) Nozoe, T. In Seventy Years in Organic Chemistry; Seeman, J. I., Ed.; *Profiles, Pathways, and Dreams: Autobiographies of Eminent Chemists*; American Chemical Society: Washington, DC, 1991.

(8) Related studies on azulenes: (a) Yasunami, M.; Kitamori, Y.; Kikuchi, I.; Ohmi, H.; Takase, K. *Bull. Chem. Soc. Jpn.* **1992**, *65*, 2127−2130. (b) Yasunami, M.; Miyoshi, S.; Kanegae, N.; Takase, K. *Bull. Chem. Soc. Jpn.* **1993**, *66*, 892−899. (c) Yasunami, M.; Sato, T.; Yoshifuji, M. *Tetrahedron Lett.* **1995**, *36*, 103−106. (d) Schuchmann, P.; Hafner, K. *Tetrahedron Lett.* **1995**, *36*, 2603−2606.

(9) Ziegler, K.; Hafner, K. *Angew. Chem.* **1955**, *67*, 301−302.

(10) (a) Hafner, K. *Liebigs Ann. Chem.* **1957**, *606*, 79−89. (b) Hafner, K.; Weldes, H. *Liebigs Ann. Chem.* **1957**, *606*, 90−99. (c) Hafner, K.; Kaiser, H. *Liebigs Ann. Chem.* **1958**, *618*, 140−152. (d) Hafner, K. *Angew. Chem.* **1958**, *70*, 419−430. (e) Hafner, K.; Pelster, H. *Angew. Chem.* **1960**, *72*, 781. (f) Hafner, K.; Moritz, K. L. *Angew. Chem.* **1960**, *72*, 918. (g) Hafner, K.; Kreuder, M. *Angew. Chem.* **1961**, *73*, 657. (h) Hafner, K.; Bernhard, C.; Muller, R. *Liebigs Ann. Chem.* **1961**, *650*, 35−41. (i) Hafner, K.; Stephan, A.; Bernhard, C. *Liebigs Ann. Chem.* **1961**, *650*, 42−62. (j) Hafner, K.; Pelster, H.; Schneider, J. *Liebigs Ann. Chem.* **1961**, *650*, 62−80. (k) Hafner, K.; Pelster, H.; Patzelt, H. *Liebigs Ann. Chem.* **1961**, *650*, 80−92. (l) Hafner, K.; Moritz, K.-L. *Liebigs Ann. Chem.* **1961**, *650*, 92−97. (m) Hafner, K.; Bangert, K.-F. *Liebigs Ann. Chem.* **1961**, *650*, 98−115. (n) Hafner, K.; Patzelt, H.; Kaiser, H. *Liebigs Ann. Chem.* **1962**, *656*, 24−33. (o) Hafner, K.; Senf, W. *Liebigs Ann. Chem.* **1962**, *656*, 34−39. (p) Hafner, K.; Moritz, K.-L. *Liebigs Ann. Chem.* **1962**, *656*, 40−53.

(11) Hafner, K.; Meinhardt, K.-P. *Organic Synthesis*; Wiley: New York, 1990; Coll. Vol. *VII*, pp 15−18.

(12) McDonald, R. N.; Richmond, J. M. *J. Org. Chem.* **1975**, *40*, 1689−1694.

(13) 2-Bromo- or 2-chlorotropone reacts with ethyl cyanoacetate to give 2-amino-1,3-carboethoxyazulene in ethanol in the presence of NaOEt. Nozoe, T.; Matsumura, S.; Murase, Y.; Seto, S. *Chem. Ind. (London)* **1955**, 1257.

(14) (a) Nozoe, T.; Seto, S.; Matsumura, S.; Asano, T. *Proc. Jpn. Acad.* **1956**, *32*, 339−343. (b) Nozoe, T.; Seto, S.; Nozoe, S. *Proc. Jpn. Acad.* **1956**, *32*, 472−475. (c) Nozoe, T.; Seto, S.; Matsumura, S.; Murase, Y. *Bull. Chem. Soc. Jpn.* **1962**, *35*, 1179−1188. (d) Nozoe, T.; Takase, K.; Tada, M. *Bull. Chem. Soc. Jpn.* **1963**, *36*, 1006−1009. (e) Nozoe, T.; Takase, K.; Tada, M. *Bull. Chem. Soc. Jpn.* **1963**, *36*, 1010−1020. (f) Nozoe, T.; Takase, K.; Shimazaki, N. *Bull. Chem. Soc. Jpn.* **1964**, *37*, 1644−1648. (g) Nozoe, T.; Seto, S.; Takase, K.; Matsumura, S.; Nakazawa, T. *Nippon Kagaku Zasshi* **1965**, *86*, 346−363; *Chem. Abstr.* **1965**, *63*, 11456e. (h) Nozoe, T.; Takase, K.; Fukuda, S. *Bull. Chem. Soc. Jpn.* **1971**, *44*, 2210−2214.

(15) Itô, S.; Tsunetsugu, J.; Kanno, T.; Sugiyama, H.; Takeshita, H. *Tetrahedron Lett.* **1965**, *6*, 3659−3663.

(16) Nozoe, T.; Kitahara, Y.; Yamane, K.; Yoshikoshi, F. *Proc. Jpn. Acad.* **1951**, *27*, 18−23.

(17) Preparation of [3,5,7-^{2}H$_3$]tropolone (**19**-d_3) and substrate **2**-d_3 was reported without description of the isotopic purities.[15] Deuteriated tropolone, **19**-d_3, was prepared from catalytic deuteriation (D_2/Pd−C) of 3,5,7-tribromotropolone[16] in dioxane−D_2O in the presence of triethylamine in 10% yield. Likewise, compound **2**-d_3 was prepared from 2-methoxy-3,5,7-tribromotropone in the presence of sodium acetate. In our examination of the above method, **19**-d_3 has been obtained with low isotopic purity (d_3, 65−84%; d_2 12−25%; d_1, 5−10%; d_0 3−6% by mass spectrometry). Hence, we need to examine a preparation of **19**-d_3 with high isotopic purity in the present work. The compound, tropolone-d_3 **19**-d_3, can be led easily to any troponoid precursors, [3,5,7-^{2}H$_3$]-2-bromotropone, [3,5,7-^{2}H$_3$]-2-chlorotropone, and [3,5,7-^{2}H$_3$]-2-tosyloxytropone, with high isotopic purity other than 2-methoxy[3,5,7-^{2}H$_3$]tropone (**2**-d_3) treated in this paper (see ref 13).

(18) Zhang, B.; Martin, M. L. *J. Am. Chem. Soc.* **1992**, *114*, 7089−7092 and references therein.

(19) Biggi, G.; Del Cima, F.; Pietra, F. *J. Am. Chem. Soc.* **1973**, *95*, 7101−7107.

(20) On the basis of the ^{13}C NMR of **5**, the structure in CD_3OD reveals the keto (tropone) form **5a** [$\delta_{C=O}$ 181.75; cf. $\delta_{C=O}$ 187.65 for tropone] rather than the enolate one (**5b**). In Table S1 (Supporting Information) the ^{13}C NMR of **5** displays 10 carbons including four singlet signals and five doublet ones. The former singlet signals are ascribed to the carbonyl carbon (C-1), two chemical-shift equivalent cyano carbons, C-9 and C-10 carbons. The predominant contribution of **5a** in solution is

supported by ^{17}O NMR spectroscopy (δ 377.61) of **5**. The ^{17}O NMR demonstrates a troponoid carbonyl carbon having an electron-donating group at C-2 position (cf. δ_O 375.03 for 2-methylaminotropone; δ_O 484.56 for the parent tropone) rather than that of the enolate structure.

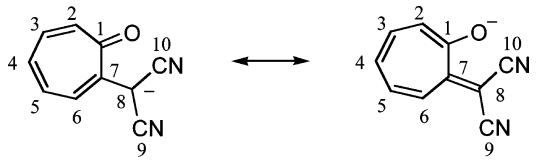

5a **5b**

(21) Machiguchi, T. *Synth. Commun.* **1982**, *12*, 1021−1025.
(22) (a) Doering, W. E.; Knox, L. H. *J. Am. Chem. Soc.* **1951**, *73*, 828−838. (b) Nozoe, T.; Seto, S.; Takeda, H.; Morosawa, S.; Matsumoto, K. *Proc. Jpn. Acad.* **1951**, *27*, 556−560.
(23) Nozoe, T.; Seto, S.; Ikemi, T.; Arai, T. *Proc. Jpn. Acad.* **1951**, *27*, 102−106.
(24) (a) Becke, A. D. *J. Chem. Phys.* **1993**, *98*, 5648−5652. (b) Lee, C.; Yang, W.; Parr, R. G. *Phys. Rev. B* **1988**, *37*, 785−789.
(25) (a) Fukui, K. *J. Phys. Chem.* **1970**, *74*, 4161−4163. (b) Gonzalez, C.; Schlegel, H. B. *J. Chem. Phys.* **1989**, *90*, 2154−2161.
(26) (a) Cancès, E.; Mennucci, B.; Tomasi, J. *J. Chem. Phys.* **1997**, *107*, 3032−3041. (b) Cossi, M.; Barone, V.; Mennucci, B.; Tomasi, J. *Chem. Phys. Lett.* **1998**, *286*, 253−260. (c) Mennucci, B.; Tomasi, J. *J. Chem. Phys.* **1997**, *106*, 5151−5158.
(27) Frisch, M. J.; Trucks, G. W.; Schlegel, H. B.; Scuseria, G. E.; Robb, M. A.; Cheeseman, J. R.; Montgomery, Jr., J. A.; Vreven, T.; Kudin, K. N.; Burant, J. C.; Millam, J. M.; Iyengar, S. S.; Tomasi, J.; Barone, V.; Mennucci, B.; Cossi, M.; Scalmani, G.; Rega, N.; Petersson, G. A.; Nakatsuji, H.; Hada, M.; Ehara, M.; Toyota, K.; Fukuda, R.; Hasegawa, J.; Ishida, M.; Nakajima, T.; Honda, Y.; Kitao, O.; Nakai, H.; Klene, M.; Li, X.; Knox, J. E.; Hratchian, H. P.; Cross, J. B.; Bakken, V.; Adamo, C.; Jaramillo, J.; Gomperts, R.; Stratmann, R. E.; Yazyev, O.; Austin, A. J.; Cammi, R.; Pomelli, C.; Ochterski, J. W.; Ayala, P. Y.; Morokuma, K.; Voth, G. A.; Salvador, P.; Dannenberg, J. J.; Zakrzewski, V. G.; Dapprich, S.; Daniels, A. D.; Strain, M. C.; Farkas, O.; Malick, D. K.; Rabuck, A. D.; Raghavachari, K.; Foresman, J. B.; Ortiz, J. V.; Cui, Q.; Baboul, A. G.; Clifford, S.; Cioslowski, J.; Stefanov, B. B.; Liu, G.; Liashenko, A.; Piskorz, P.; Komaromi, I.; Martin, R. L.; Fox, D. J.; Keith, T.; Al-Laham, M. A.; Peng, C. Y.; Nanayakkara, A.; Challacombe, M.; Gill, P. M. W.; Johnson, B.; Chen, W.; Wong, M. W.; Gonzalez, C.; Pople, J. A. *Gaussian 03, Revision C.02*; Gaussian, Inc.: Wallingford, CT, 2004.